

Physics of Wave Processes and Radio Systems

2025, vol. 28, no. 1, pp. 56–75

DOI [10.18469/1810-3189.2025.28.1.56-75](https://doi.org/10.18469/1810-3189.2025.28.1.56-75)
UDC 537.87
Original Research

Received 28 November 2024
Accepted 28 December 2024
Published 31 March 2025

Antenna-feeder systems for EHF radio interferometers

Ekaterina Yu. Gaynulina , *Vladimir N. Ikonnikov* ,
Nikolay S. Kornev , *Andrey V. Nazarov* , *Yuriy I. Orekhov*

Russian Federal Nuclear Centre – All-Russian Research Institute of Experimental Physics
37, Mira Avenue,
Sarov, Nizhny Novgorod Region, 607188, Russia

Abstract – Background. The development of a microwave method for researching shock-wave and detonation processes using radio interferometers requires the development of antenna-feeder systems taking into account the specifics of gas-dynamic experiments. **Aim.** Design of antenna-feeder systems for radio interferometers in the millimetre and submillimetre wavelength ranges, development of options for constructing feeder lines and probing devices. **Methods.** The results of numerical modelling in CST MWS, theoretical calculations and experimental studies of interferometer antenna-feeder systems are presented, confirming the effectiveness of the proposed technical solutions. **Results.** The requirements for antenna-feeder systems as an integral part of the radio interferometer are given. The advantages of dielectric emitters are justified and planar dielectric emitters are proposed. Small-sized antenna-feeder systems with dielectric inserts are proposed, which have found their application in diagnostic tasks in closed volumes. In order to reduce losses in the feed line and build lines up to several metres, antenna-feeder systems on rectangular supersized metal waveguides have been studied, including the proposed pyramidal horn transitions from standard waveguide section to a supersized section, and a combined feeder line using a fixable dielectric waveguide to connect metal waveguides. A quasi-optical two-mirror antenna with high spatial resolution and minimal losses is considered. **Conclusion.** The article shows the advantages of the microwave diagnostic method, various methods and schemes for constructing feeder lines, and justifies the use of different types of probing devices (emitters) depending on the problem being solved and the operating frequency range.

Keywords – radio interferometer; antenna-feeder system; probing devices; dielectric waveguide; supersized waveguide; quasi-optical antenna.

Introduction

Currently, the microwave diagnostics method has firmly established itself among modern methods for studying shock-wave and detonation processes. The results obtained using microwave diagnostics significantly expand the information content, as well as the possibilities and prospects for studying the properties of substances and materials under intense dynamic influences.

Important advantages of the method are its remoteness and non-perturbing nature, and, compared to laser interferometric systems, the ability to continuously record the movement of shock and detonation waves in optically opaque materials, which include virtually all solid high-energy materials and many polymer materials used in research as barriers and screens. The characteristic dimensions of the roughness of reflective surfaces, such as the roughness of the detonation front or the surfaces of impactors and shells, are significantly smaller than the wavelength of microwave radiation.

Thus, for microwave radiation, such surfaces are almost smooth, whereas for the laser method, they

are diffusely reflective, which creates problems in interpreting the results of laser diagnostics [1].

The surge in the development of microwave technology in the early 2000s led to the improvement of the design of radio interferometers (RI) in the millimetre (mm) wavelength range and methods for recording and processing experimental data, which made it possible to move to a completely new level of quality in the study of fast-flowing processes [2]. The Y.E. Sedakov Research Institute of Measurement Systems (RIMS) has developed a series of RIs designed to measure the kinematic and reflective characteristics of fast-flowing processes. Thus, work [3] presents some results of the application of interferometers in the 8- and 3-mm wavelength ranges.

The creation of the single-channel RI-03 three-millimetre range radioisotope (Fig. 1) made it possible to begin a whole cycle of work on microwave diagnostics of fast-flowing processes, to develop and master new methods of radio wave measurements that were previously unavailable.

This was made possible by the high energy potential of the transceiver (over 60 dB), the short operating wavelength (3.2 mm), which is significantly shorter than that of previous analogues, and the wide range



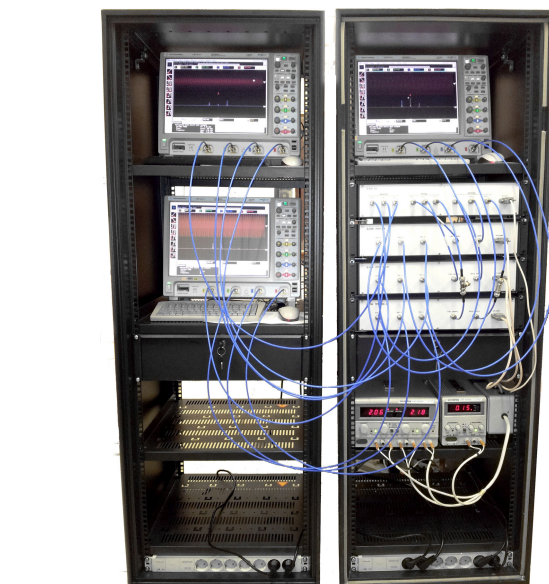
Fig. 1. Single-channel interferometer of the three-millimetre range RI-03
Рис. 1. Одноканальный интерферометр трехмиллиметрового диапазона РИ-03

of speeds that can be recorded: from fractions of a millimetre per second to 10 km/s.

However, despite its undoubted advantages, the RI-03 radio interferometer had its drawbacks. The energy potential of the device was limited due to the presence of strong “backlighting” at the receiver input, caused by the direct passage of a powerful transmitter signal to the receiver. Backlighting occurred due to the imperfect matching of the waveguide circuits inside the device with the antenna-feeder system (AFS).

The design flaws of the RI-03 radio interferometer were taken into account in the development of the MRI-03 multichannel radio interferometer (Fig. 2, a) and the PRI-03 radio interferometer. Along with the information about motion obtained using single-channel RI, the MRI-03 solved the problem of reconstructing the shape of objects' surfaces and the dynamics of their changes over time. With the help of the developed PRI-03 in active-passive mode, measurements of the kinematic (radio interferometric mode) and thermal (radiometric mode) characteristics of fast-flowing processes were simultaneously implemented. In this case, the device is a microwave radio interferometer-radiometer (Fig. 2, b).

The advantages of the microwave sounding method initiated the further development of microwave radio interferometry and the transition to shorter wavelengths – in the submillimetre range (submm), which allows for increased accuracy and resolution of measurements of the displacements and velocities of the diagnosed objects.



a



b

Fig. 2. External appearance of radio interferometers MRI-03 (a) and PRI-03 (b)
Рис. 2. Внешний вид радиоинтерферометров МРИ-03 (а) и ПРИ-03 (б)

1. Antenna-feeder system as a component of a radio interferometer

When considering the design schemes of radio interferometers and the methods of measurement carried out with their help, an important issue is the transmission of probing radiation from the radio interferometer to the object under study.

The main requirements for waveguide systems are related to minimising radiation transmission losses, as well as reducing cost and ease of use. The conditions of the gas-dynamic experiment also impose restrictions on the choice of AFS for use in RI. Thus, the AFS must ensure:

- placement of measuring equipment behind a protective barrier, out of direct view of the object under study, i.e. length and flexibility of the path;



Fig. 3. External appearance of the dielectric waveguide
 Рис. 3. Внешний вид диэлектрического волновода



– minimal losses during the transmission of probing and information signals.

The following requirements are imposed on the AFS emitter:

- formation of radiation with high spatial resolution;
- the main lobe of the irradiator's directional pattern to be covered by the object under investigation;
- low background radiation level.

2. Dielectric feeder line – reasons for selection and construction options

Hollow metal waveguides (MW) and dielectric waveguides (DW) can be used to transmit probing radiation [3; 4].

The latter are widely used in the AFS of various EHF transceivers to transmit probing radiation from the interferometer to the experimental assembly due to their low cost compared to other types of waveguides (in the frequency range under consideration) and ease of use (simple implementation of radial bends).

2.1. Dielectric line of the three-millimetre wavelength range

A variant of the 3 mm wavelength waveguide line is DW, which is a $2,2 \times 1 \text{ mm}^2$ fluoroplastic sheet in a polyethylene foam shell, placed in an outer corrugated PVC shell (Fig. 3).

The specified cross-section size of the waveguide ensures single-mode propagation of the main wave NE_{11} and line loss of no more than 2 dB/m , which allows the use of waveguides up to 10 m long. At the same time, waveguide bend radii of at least 20λ are permissible, with virtually no change in phase shift.

To use the described waveguide as part of a transmission line (TL) in the RI path, it must be matched to the receiving input. For this purpose, smooth

waveguide transitions from the waveguide to a rectangular waveguide with a standard cross-section of $2,4 \times 1,2 \text{ mm}^2$ can be used [5].

The most obvious solution in terms of matching the antenna to the waveguide is to use the open end of the waveguide itself as an antenna (Fig. 3). To study its directional properties, numerical modelling of the directional pattern (DP) and experimental measurements of the amplitude distribution (AD) of the field in the polarisation plane of the main wave NE_{11} were carried out. In the CST MWS package, the RD for the open end of the waveguide made of PTFE-4 with $\epsilon = 2,2$, $\text{tg}\delta = 2 \cdot 10^{-4}$ was obtained, and the simulation was performed at the operating frequency $f = 92,5 \text{ GHz}$. The RD in the polarisation plane of the fundamental wave is shown in Fig. 4.

As can be seen from Fig. 4, the open end of the waveguide is a wide-directional antenna with a main lobe width of minus 3 dB $28 = 33^\circ$. The maximum level of the side lobes is minus 17,1 dB, which allows them to be ignored in the conditions of the tasks being solved.

As noted in the antenna requirements, the main lobe of its radiation pattern must be covered by the object under study.

Due to the wide directivity of the antenna, the minimum dimensions of the object under investigation can be calculated using the width of the main lobe of the DW at a level of minus 10 dB, which is $20 = 65^\circ$, then the dimensions of the object under investigation should be determined by the ratio: $R_{06} > \text{rtg}(\theta)$, where R_{06} is the radius of the object under investigation; r is the distance from the aperture to the object under investigation; θ is the angular size of half the width of the main lobe of the open end of the antenna at a level of minus 10 dB. For example, when the object is removed from the antenna to a distance of up to 100 mm, its radius must be at least 64 mm.

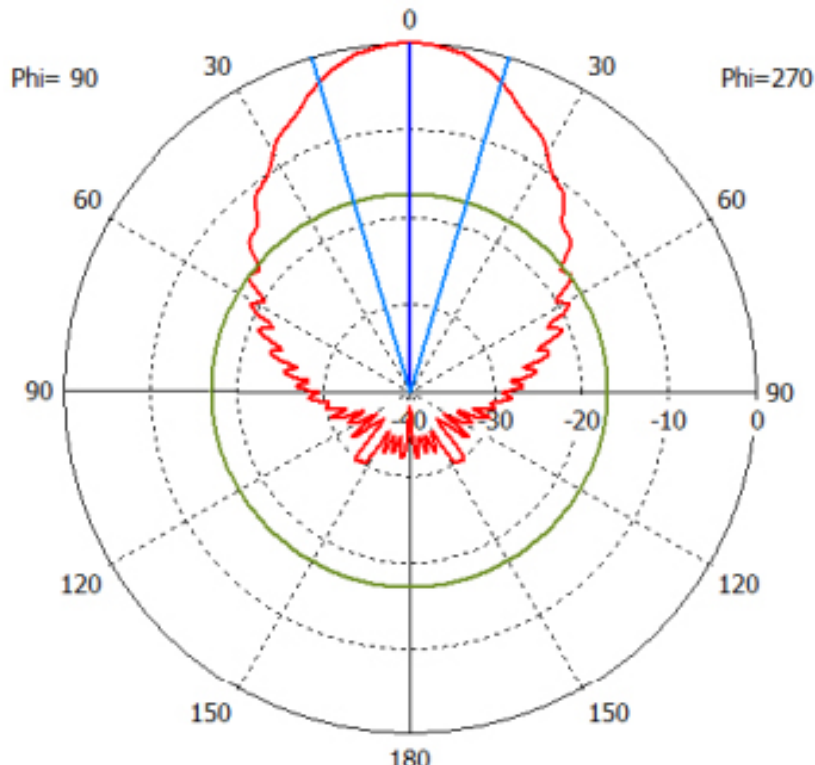


Fig. 4. Directional diagram of the open end of the DW (CST MWS)
Рис. 4. Диаграмма направленности открытого конца ДВ (CST MWS)

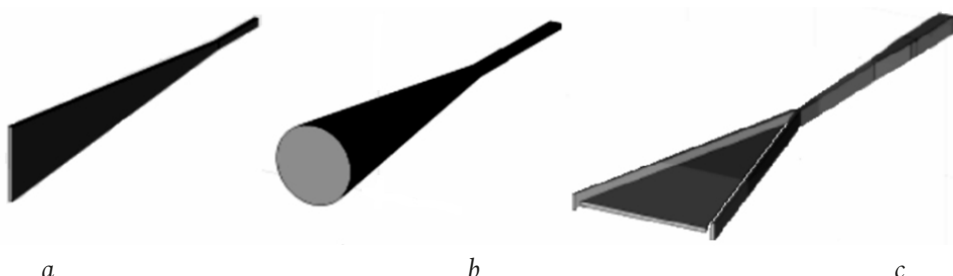


Fig. 5. Designs of conical (b) and planar emitters (a, c)
Рис. 5. Конструкции конического (б) и планарных излучателей (а, в)

This estimate of the dimensions of the object under study is valid only when probing in a vacuum; when probing in a dielectric medium, the main lobe of the open end of the antenna is narrower.

2.2. Dielectric planar emitters in the three-millimetre range

To solve the problems of multichannel interferometry (MRI), due to their specificity, it was necessary to create waveguide emitters based on multimode waveguides [6]. For typical conditions of such tasks, the objects of study and the range of their movements are characterised by dimensions of tens of wavelengths. These conditions are characterised by the diffractive nature of wave radiation in the Fresnel zone. Taking into account the diffraction nature of the formation of probing radiation and its interaction with the di-

agnostic object, characteristic of gas-dynamic experiments, the need to form probing radiation in the form of Gaussian wave beams was justified [7].

Dielectric conical and planar wedge-shaped emitters have been proposed, which, on the one hand, ensure the narrowing of the beam by increasing the cross-sectional size of the antenna at the aperture, and on the other hand, ensure the formation of Gaussian wave beams (Fig. 5). The designs of the emitters are protected by Russian Federation patents [8–10].

Below are some results of numerical modelling in CST MWS and experimental studies on a metrologically certified test bench of the RIMS for emitter structures shown in Fig. 5.

A conical radiator (Fig. 5, b) provides axisymmetric radiation. Since multi-channel RI requires resolution in the transverse coordinates, wedge-type radiators

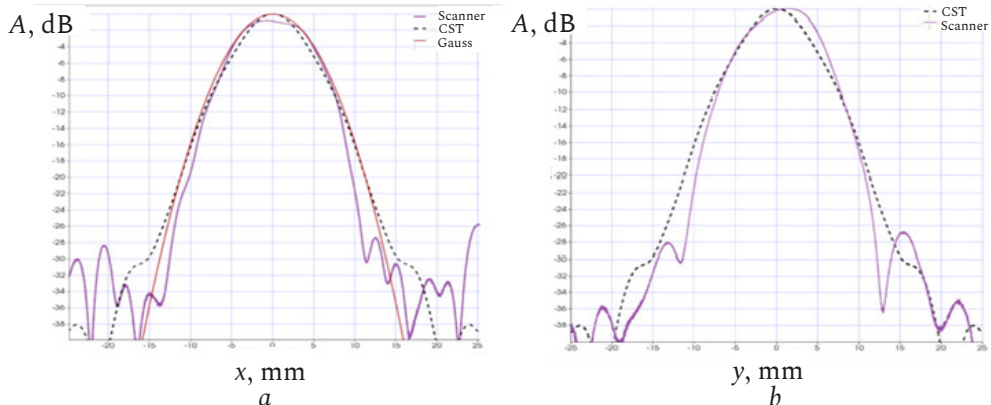


Fig. 6. Amplitude distributions of the field component E_y of a conical emitter at a distance of 10 mm (a – in the H-plane; b – in the E-plane)

Рис. 6. Амплитудные распределения составляющей поля E_y конусного излучателя на расстоянии 10 мм (а – в Н-плоскости; б – в Е-плоскости)

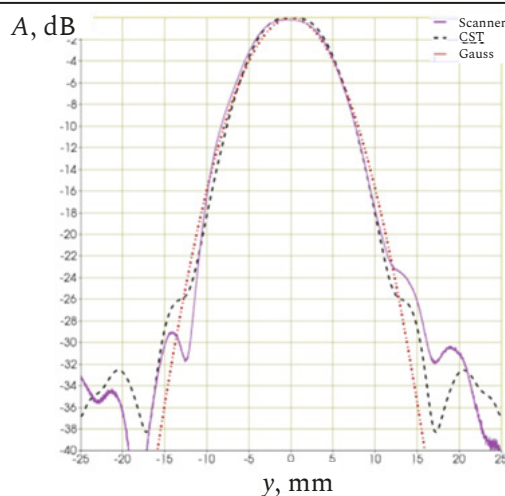


Fig. 7. Amplitude distributions of the field component E_y of a wedge-shaped emitter in the E-plane at a distance of 10 mm between the planes of the emitter and probe apertures (E-plane)
Рис. 7. Амплитудные распределения составляющей поля E_y клиновидного излучателя в Е-плоскости на расстоянии 10 мм между плоскостями апертур излучателя и зонда (Е-плоскость)

with excitation from the apex by a single-mode RFW (Fig. 5, a), as well as with two-input excitation by distributed coupling DV with a wedge along its side edges (Fig. 5, c). These emitters have also found application in single-channel RI.

The results of experimental studies and numerical CST modelling of wedge-shaped emitters over a wide range of parameters are presented in [11].

The larger side of the $2b$ aperture cross-section of the emitter was selected within a wide range of sizes $(2-10)\lambda$, characteristic of the multimode mode of the DV. The size of the smaller side of the $2a$ cross-section = $0,3125\lambda$, characteristic of the single-mode mode. The emitter was made of fluoroplastic ($\epsilon = 2,08$). The wedge angle is 10° , measurements were taken at $\lambda = 3,2$ mm.

To illustrate the results of experimental studies, Figures 6 and 7 show the AP of the *E*-field component

for conical and wedge-shaped emitters, respectively. For ease of comparison, the size of the larger side of the cross-section at the aperture of the wedge-shaped emitter and the diameter at the aperture of the conical emitter are taken to be the same, equal to 16 mm (5X). For comparison, the results of numerical simulation in CST and the calculated AFR of the main mode of the Gaussian-Hermite wave packet (PGE_0) are given.

The presented AR dependencies show that conical emitters (Fig. 6) are characterised by the presence of side extremes at the level of minus 15...20 dB. Nevertheless, wedge-shaped emitters can be used in single-channel IR systems provided that the transverse dimensions of the irradiation area OD do not exceed the AFR width at a level below minus 30 dB.

Experimental studies of the wedge-shaped emitter field have shown that the level of the side lobes is less than minus 25 dB, and the AR has a beam-like character, but differs from the Gaussian function (Fig. 7). Thus, the problem of the influence of AFR unevenness in the direction of the axis on the accuracy of measurements remains.

To expand the capabilities of diagnostics and MRI tasks, it is essential to form PGE_0 . In this case, the field distribution has no zeros, which eliminates the error in measuring displacements due to phase jumps characteristic of the field distribution with side lobes. In addition, the simplest analytical description of PGE_0 ensures high-precision MRI signal processing.

Although wedge-shaped emitters can be used in single-channel MRI, provided that the transverse dimensions of the irradiation area of the diagnostic object do not exceed the AFR width at a level below minus 30 dB, such an emitter provides limited possibilities for controlling the amplitudes of higher modes at the aperture, and therefore for forming PGE_0 with the required accuracy. This is due to the

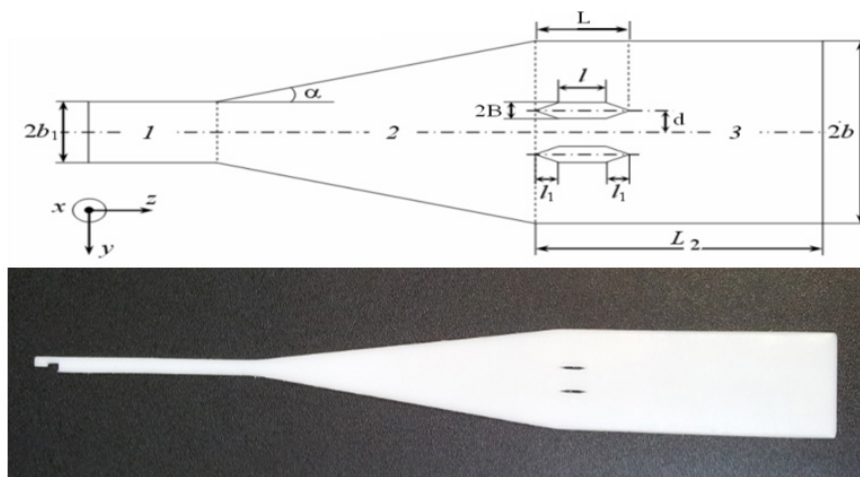


Fig. 8. Structure and appearance of the experimental sample of the emitter with inhomogeneities in the form of wedge-shaped slits
 Рис. 8. Структура и внешний вид экспериментального образца излучателя с неоднородностями в форме клиновидных щелей

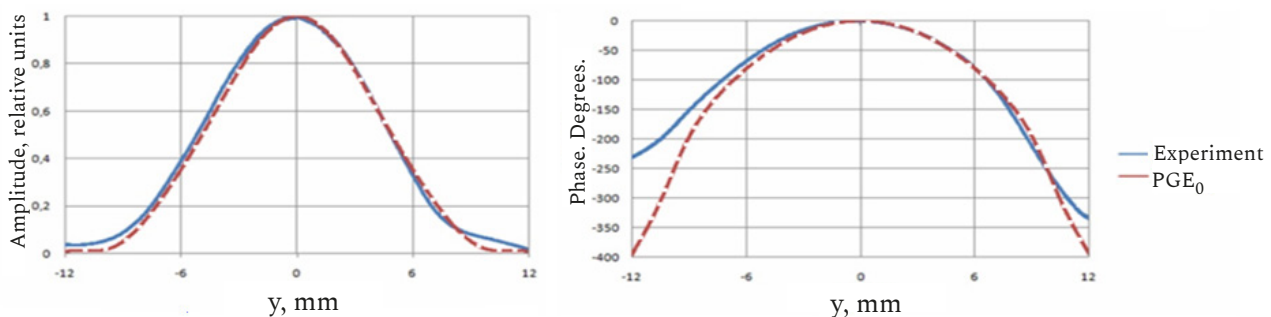


Fig. 9. Experimental amplitude and phase distributions of the component E_y of the electric field in comparison with the PGE_0 at a distance of 20 mm from the aperture
 Рис. 9. Экспериментальные амплитудные и фазовые распределения составляющей E_y электрического поля в сравнении с PGE_0 на расстоянии 20 мм от апертуры

fact that the choice of transition parameters is primarily determined by the need to ensure minimum losses (the “adiabaticity” condition). In this case, the transition profile is linear, as a result of which the conversion of modes at the transition is characterised by deformation of the excitation field structure, and the conversion to higher modes is negligible.

An effective technical solution [12; 13] for an emitter based on a section of a wide-format rectangular waveguide (WRFW) with a wedge-shaped transition from a single-mode waveguide (Fig. 8) has been proposed. In a plane parallel to the wide edges of the waveguide, the width of the cross-section of the probing field can be significantly narrowed compared to the single-wave mode field in another plane.

The wedge 2 acts as a smooth transition from the single-mode waveguide 1 to the multi-mode waveguide 3. The WRFW-based illuminator forms a probing field with independent control of the field’s AFR in two orthogonal directions. The ability to control the AFR of the WRFW end face radiation is provided in multimode mode by means of controlled summation of eigenmodes with specific amplitudes.

A method is proposed for implementing the mode composition of WRFW fields required for PGE_0 synthesis.

The AFR of the radiation field at the end of the regular section of the WRFW is approximated by PGE_0 based on the waves NE_{11} , NE_{13} , NE_{15} of the WRFW. The task of exciting the required set of higher modes with specified amplitude-phase ratios and controlling the mode composition is solved by introducing local inhomogeneities on a section of the regular WRFW.

To minimise the level of reflections from the inhomogeneities introduced into the RFW section and to ensure the minimum possible root mean square deviation (RMS) of the emitted beam from PGE_0 , it is proposed that the slits be made in the form of hexagons elongated along the axis (Fig. 8). Based on the design results, emitter structures were manufactured, variants of which are protected by a Russian Federation patent [14]. The synthesised AFR PGE_0 practically coincides with the results of numerical modelling in the CST MWS program in the distance range from 20 to 100 mm. Figures 9 and 10 also show the experimen-

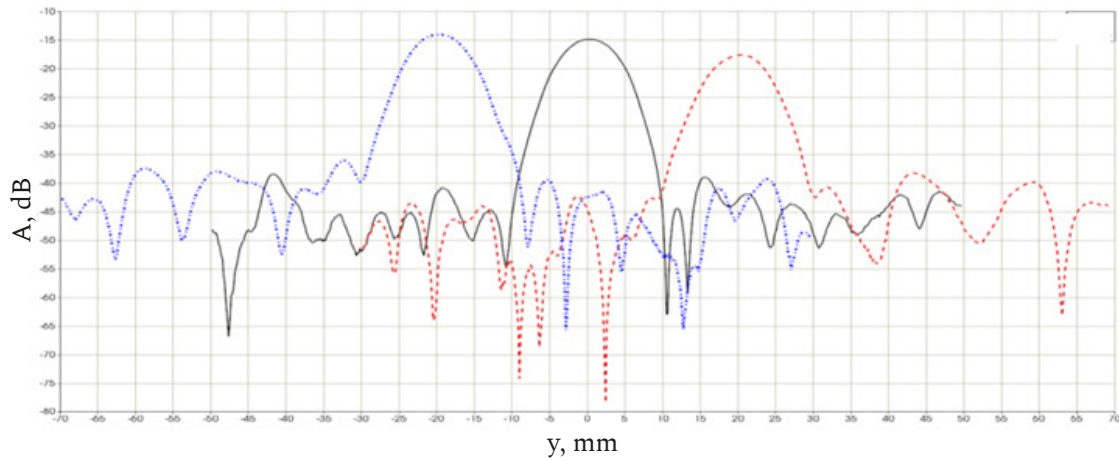


Fig. 10. Experimental AR $E_y(y)$ in the E-plane for a three-channel system of emitters
 Рис. 10. Экспериментальные АР $E_y(y)$ в Е-плоскости для трехканальной системы излучателей

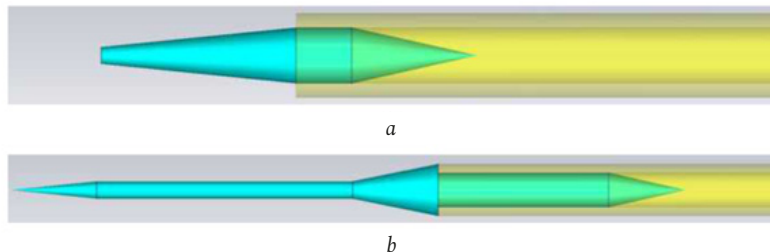


Fig. 11. Variants of rod dielectric emitters: a – with a thickness equal to the diameter of the MW and a truncated point; b – with a thickness less than the diameter of the MW, with a stepwise change in the radius of the section
 Рис. 11. Варианты стержневых диэлектрических излучателей: а) с толщиной, равной диаметру МВ и усеченным заострением; б) с толщиной, меньшей диаметра МВ, со скачкообразным изменением радиуса сечения

tal amplitude and phase distributions formed by the emitter, measured at a distance of 20 mm from the aperture, in comparison with the AFR PGE₀ also show the experimental amplitude and phase distributions of the probing beam formed by the emitter, measured at a distance of 20 mm from the aperture, and the AR of a three-channel emitter system measured at the same distance for use in multichannel diagnostics. Up to a level of minus 35 dB, the AR coincide with the PGE₀ with a standard RMS of no worse than 10⁻³.

The developed emitters are part of single-channel and multi-channel RI and are used in the diagnostics of gas-dynamic processes.

3. Small-sized AFS with dielectric inserts

There are a number of tasks that require the diagnosis of gas-dynamic processes in closed

volumes with limited free space inside. Such applications require emitters with minimum dimensions that form an axisymmetric DN with a width of no more than 40° at a level of 0,5, ensuring amplitude and phase distributions of the radiation field within the required area of the surface moving in the diagnosed closed volume and ensuring a minimum level of side lobes (SL).

The requirement for such a small probing beam width with a D / λ ratio of no more than 3, which is unfeasible for metal waveguide emitters, can also be met by using dielectric emitters, in which the formation of the beam pattern is ensured by a physical aperture exceeding the geometric one.

Work [15] presents the results of research and design of small-sized AFS UHF RI emitters that would meet the requirements. The AFs must ensure the formation of radiation in the three-millimetre wavelength range ($\lambda = 3,2$ mm) through an opening in a fluoroplastic screen. An MW with an internal cross-section of 2 mm is used as the feed line for the AFS being created, and the external diameter of the MW is selected to be 3 mm for technological reasons.

Due to the specificity of DWs as open systems, the directivity of wave-guiding dielectric elements (rod, cone, etc.) is determined by the cross-section of the wave power distribution NE₁₁ with a field drop at the cross-section boundary of 15-20 dB. Therefore, it was proposed to place a coaxial dielectric radiator with external nozzle dimensions of no more than 10 mm in the longitudinal and transverse coordinates at the open end of the MW.

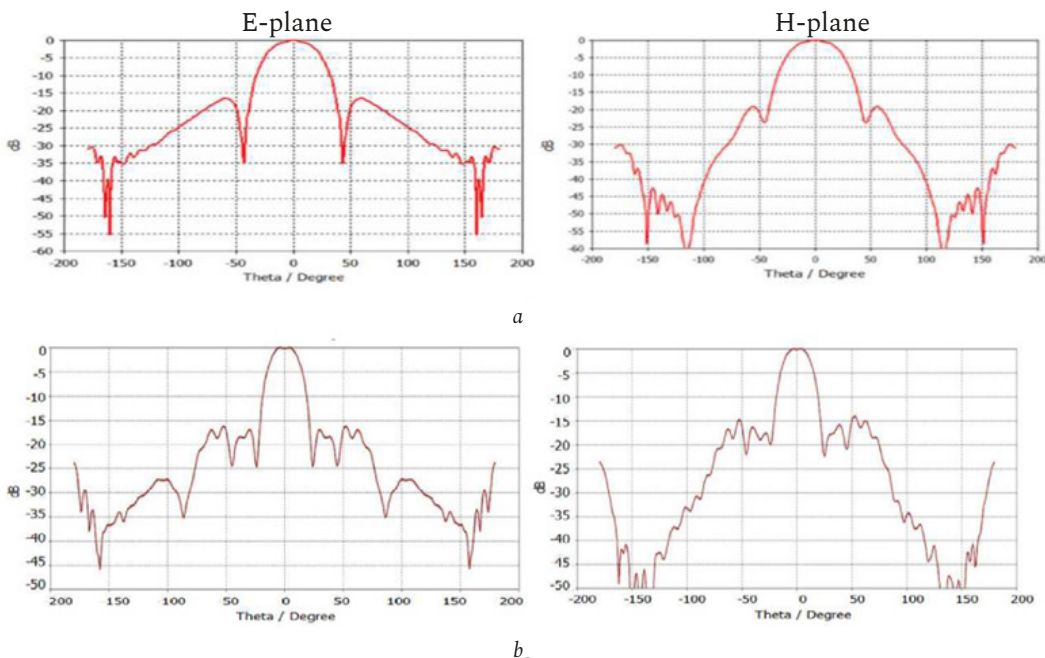


Fig. 12. Directional pattern formed by a polystyrene rod radiator shown in: a – Fig. 11, a; b – Fig. 11, b
 Рис. 12. Диаграмма направленности, формируемая стержневым излучателем из полистирола, представленным на: a – рис. 11, a; б – рис. 11, б

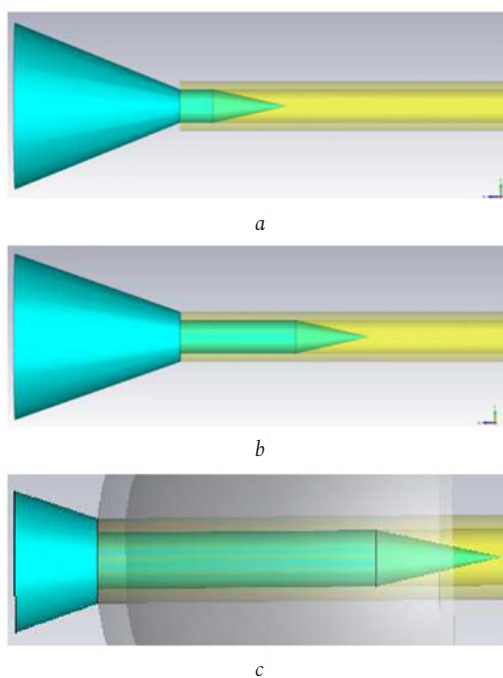


Fig. 13. Variants of a dielectric conical emitter
 Рис. 13. Варианты диэлектрического конического излучателя

Designs for dielectric AFS radiators have been proposed, and numerical simulation results for them have been obtained using the CST MWS programme.

3.1. Rod dielectric radiator

The rod radiator is made in the form of a pin made of polystyrene or quartz with a smooth conical taper. The thickness of the rod is chosen to be equal to

(Fig. 11, a) or less than (Fig. 11, b) the inner diameter of the MW, and the length of its outer (radiating) part is 10 mm.

For emitters of this type, the physical aperture depends on their thickness and material. For example, according to the results of modelling a design with a polystyrene rod with a diameter of 2 mm, equal to the inner diameter of the MW (Fig. 11, a), an almost symmetrical beam with a SL of minus 16,6 dB was obtained. The beam width was 41,9° and 43,6° in two planes, respectively (Fig. 12, a). The maximum length of the emitter should be considered to be 7 mm. Further shortening leads to an expansion of the beam width and an increase in the SL.

A distinctive feature of this design variant (Fig. 11, b) is the smooth transition from a rod with a diameter of 2 mm, equal to the inner diameter of the MW, to a thin rod with a diameter of 1 mm.

The length of the smooth transition was chosen to be (4–5) mm. The length of the outer part of the emitter is 25 mm.

The introduction of a conical transition with a step change in the cross-section radius at the output of the MW, equal to 0,5 mm (Fig. 11, b), improves the matching, thereby reducing the SL to a value of minus 14,3 dB when a narrow DN is reached (Fig. 12, b).

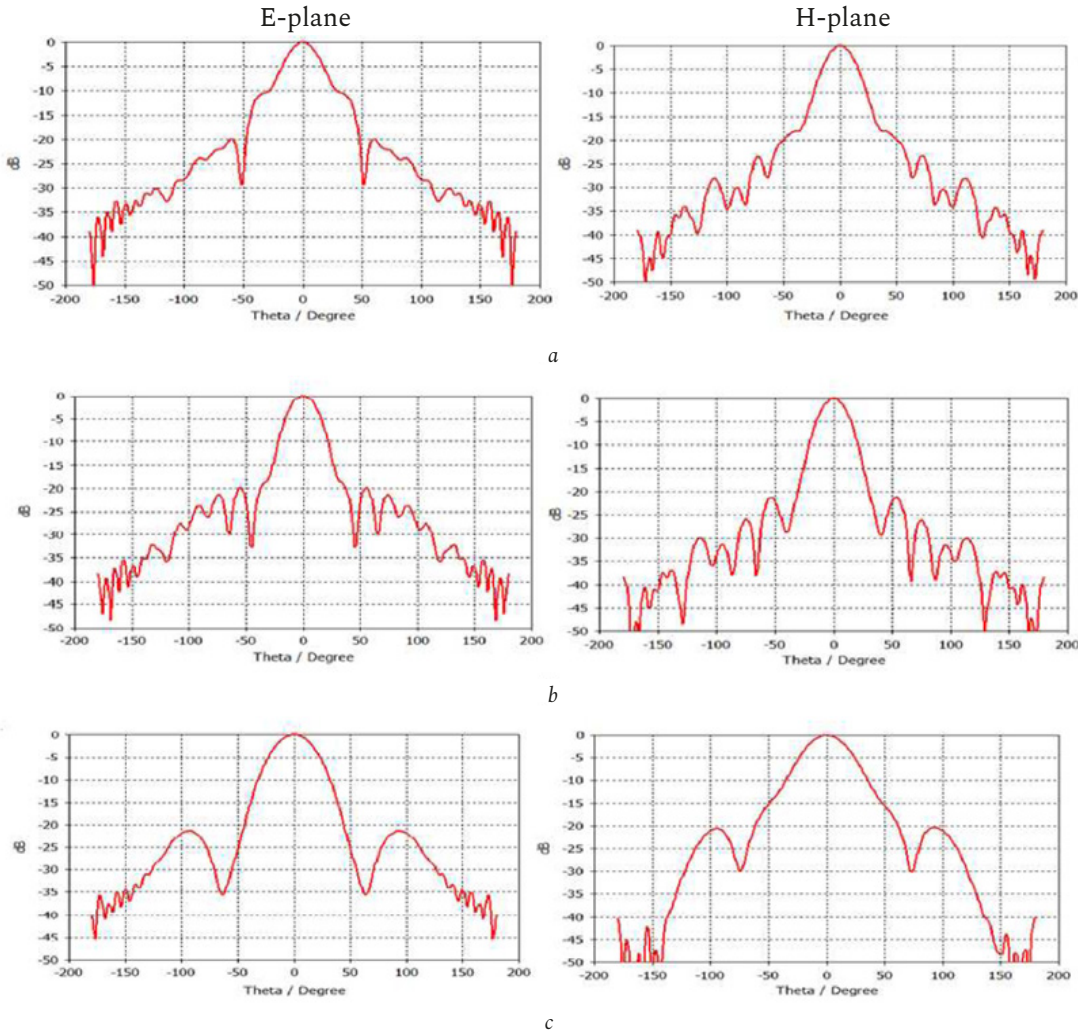


Fig. 14. Directional patterns formed by a conical polystyrene radiator shown in: a – Fig. 13, a; b – Fig. 13, b; c – Fig. 13, c
 Рис. 14. Диаграммы направленности, формируемые коническим излучателем из полистирола, представленным на: а – рис. 13, а; б – рис. 13, б; в – рис. 13, в

3.2. Dielectric conical radiator

The proposed conical radiator has a length and aperture diameter of 10 mm. The cone is a continuation of the dielectric pin inserted into the MW (Fig. 13).

The radiation pattern formed by the conical polystyrene radiator (Fig. 13, a) is shown in Fig. 14, a. A practically symmetrical narrow-beam wave beam with a level of minus 10 dB and a field distribution close to Gaussian was obtained. The width of the directivity pattern in the E and H planes is 26,5° and 24,9°, respectively. The SL does not exceed minus 20 dB.

It is known [16] that emitters, at the output of which a wave beam is formed in the form of the main Gaussian-Hermite mode, provide significantly greater accuracy of radio interferometric measurements in the diagnosis of gas-dynamic processes due to a significant reduction in the level of side lobes. It has been noted [6] that one way to form a Gaussian field distri-

bution at the emitter aperture is to excite the higher mode in a certain ratio to the fundamental mode.

A design with a sharp irregularity in the form of a step change in the diameter of the dielectric element at the output of the MW from 2 mm to 3 mm (Fig. 13, b) has been proposed. At the sharp irregularity, a wave of the highest symmetric type EN₁₂ is effectively excited and, in combination with the fundamental wave NE₁₁, it ensures the formation of a Gaussian-type DN. The modification of the design made it possible to obtain significantly better radiation parameters compared to a dielectric cone without an abrupt change in the cross-section diameter: the DN width was 24,8° in the E-plane and 23,4° in the H-plane, Gaussian distribution of the wave beam field is observed up to a level of minus 19 dB at SL not exceeding minus 21 dB (Fig. 14, b). With more stringent requirements for the external dimensions of the emitter, it is possible to further reduce the dimen-

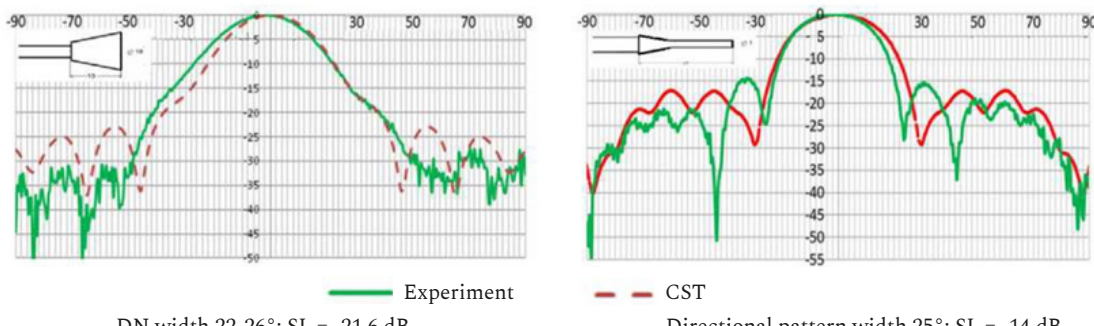


Fig. 15. Experimental AR of small-sized emitter samples in comparison with CST modelling results
 Рис. 15. Экспериментальные АР образцов малогабаритных излучателей в сравнении с результатами моделирования CST

sions to an aperture of 5 mm and a length of the outer conical part of 2,85 mm (Fig. 13, c), which will give a beam width expansion of no more than 10° without deteriorating the SL (Fig. 14, c).

The results of experimental studies at a frequency of 93,7 GHz using two optimal samples of small-sized AFS emitters are summarised in Fig. 15. They are in good agreement with the simulation results, which confirms the possibility of using the selected variants of dielectric AFS emitters for a wide range of radio interferometric probing tasks, including in conditions of strict requirements for AFs dimensions when installed inside measuring units, the free space inside which is limited.

Conical emitters with an aperture diameter of 10 mm achieve the minimum (among the small-sized models studied) width of the DN. For use in RI when probing objects in both open and closed volumes, an emitter with a shortened conical insert with a step change in cross-sectional diameter should be selected, in which parasitic side radiation practically does not irradiate the probed surface – in the DN formed by it, the minima of the main lobe are in the region of angles + (60 70)°, and the first side lobe has a maximum in the direction of angles + (90 100)° relative to the direction of the maximum of the main lobe.

This property will help avoid multiple reflections that distort the result.

The proposed variants of dielectric EHF RI emitters made it possible to ensure narrow radiation and SL, which are unattainable when using metal waveguide and horn emitters of the same size.

4. Low-loss transmission lines on an oversized metal waveguide

As already noted, one solution to the problem of improving the measurement accuracy and dynamic properties of the EHF radiometer is to reduce losses in the AFU. The specifics of gas-dynamic experiments

require the transceiver to be placed at a safe distance from the measurement object, and the antenna to be placed in close proximity to it. The waveguides used in gas-dynamic experiments, which have linear losses of about 2,5 dB/m, limit the length of the waveguide path for use in an EHF RI to no more than 2 m. A further increase in the length of the waveguide leads to an increase in losses in the waveguide path and a decrease in the ratio of the useful signal power to the noise power at the output of the measuring system.

The task of reducing losses in waveguides, especially in the mm and sub-mm wavelength ranges, is extremely important [17]. Currently, ribbon waveguides [18], quasi-optical beam mirrors and other similar guiding structures [19; 20] are known, which have line losses of less than 0,1 dB/m in the mm wavelength range. However, these waveguides have disadvantages: ribbon waveguides do not allow bends, touches, or inhomogeneities in the dielectric fabric, and quasi-optical mirror waveguides require precision adjustment. Therefore, the use of these waveguides in gas-dynamic experiments as part of an EHF radiometer waveguide may be difficult.

A well-known class of low-loss waveguides are supersized metal waveguides (SSMW) with rectangular and circular cross-sections [21; 22], which, with a ratio of waveguide cross-section D to wavelength λ equal to $D/\lambda = 5...20$, provide line losses that are an order of magnitude lower than in single-mode rectangular waveguides of standard cross-section.

When designing waveguides on OWWM, it is necessary to take into account the multimode wave propagation mode. The number of possible wave types is proportional to S/X , where S is the cross-sectional area of the waveguide. For this reason, sharp irregularities are unacceptable in waveguides on SSMW, and the optimal excitation of such waveguides in accordance with the principles of quasi-optics is provided by a

Gaussian wave beam with a ratio of beam width w (at level 0,5) to waveguide diameter D $w/D = 0,5...0,6$.

4.1. Transmission lines on a rectangular oversized metal waveguide

The simplest option for implementing LP on SSMW is a line on a rectangular SSMW.

The line losses for the fundamental wave H_{10} in a rectangular SSMW with a standard cross-section of $7,2 \times 3,4 \text{ mm}^2$, which is oversized at the operating wavelength of the UHF RI transmitter $X = 3,2 \text{ mm}$, have been calculated. According to the simulation results, the value of line losses at the operating wavelength $X = 3,2 \text{ mm}$ was $0,76 \text{ dB/m}$.

A smooth pyramidal horn transition with a cross-section of $2,4 \times 1,2 \text{ mm}^2$ to $7,2 \times 3,4 \text{ mm}^2$ and a length of 30 mm ($\sim 10X$) was selected as the LP exciter on the SSMW. The results of its modelling showed that the waveguide transition in the frequency range from 90 to 100 GHz has a VSWR value not exceeding 1,15, an average attenuation of 0,09 dB, and is a reciprocal device, which allows it to be used as part of an LP. For experimental study of line losses in a rectangular SSMW, 0,5 m long sections were made from a standard pipe, and for their excitation, smooth pyramidal horn transitions with a cross-section of $2,4 \times 1,2 \text{ mm}^2$ to $7,2 \times 3,4 \text{ mm}^2$ 30 mm long ($\sim 10X$) (Fig. 16).

Attenuation measurements in four variants of waveguide assemblies showed that the VSWR did not exceed 1,14 in all cases. The experimental value of the line loss in the manufactured rectangular SSMW with a cross-section of $7,2 \times 3,4 \text{ mm}^2$ in the working frequency band of the UHF RI is $0,8 \text{ dB/m}$, which is close to the simulation results and the theoretical value. The difference is explained by the limited accuracy of the numerical model during simulation, the instrumental error of the panoramic meter, and unaccounted losses due to various inhomogeneities present in the actual waveguide.

In particular, [23] notes that at high frequencies, the determining factor affecting waveguide characteristics is the quality of processing (roughness) of shielding surfaces. Using the considered LP, made on rectangular SSMWs, it becomes possible to place the UHF RI transceiver unit at a distance of up to 9 m from the experiment site while maintaining sensitivity at a level comparable to that provided when using a DV no more than 2 m long.

This solution has a number of disadvantages. The rigid design of waveguide connections does not allow waveguides to be bent, so the UHF RI transceiver unit will have to be placed in direct line of sight from

the object of study on a straight section, which will require additional measures to protect it from the effects of a direct shock wave. Another disadvantage is the high cost of manufacturing SSMWs (especially with silver coating). Therefore, the use of SSMWs is advisable in laboratory conditions.

4.2. Combined transmission line on a rectangular SSMW and DV

An obvious solution to ensure the safety and integrity of the transceiver unit is to use flexible DWs in conjunction with SSMWs. The section where the waveguide bend is required is made of DW, and the regular section is made of rectangular SSMW.

To implement the possibility of using rectangular SSMWs in the composition of the UHF RI LP, a flexible waveguide option was proposed for connecting MWs of standard and oversized cross-sections [24], a sketch and experimental sample of which is shown in Fig. 17.

The area of the oversized section at the output of waveguide transition 2 should be determined from the ratio $S/\lambda^2 = 2...8$, where λ is the operating wavelength. In this case, the length of the expanding section of the waveguide channel should be at least 6λ . With this design of waveguide transition 2, minimal conversion of the fundamental wave H_{10} of the rectangular MW into higher wave types is ensured due to the concentration of the electromagnetic field of the fundamental wave inside the wedge-shaped section of the DV and its effective conversion into the fundamental wave NE_{11} of the DV.

Similarly, when the wave NE_{11} propagates along DV, the reverse conversion of the wave NE_{11} into N_{10} occurs in waveguide transition 3.

To quantitatively assess the attenuation and matching quality of the DV with the SSMW at transition 2, numerical modelling of attenuation and VSWR was performed in both directions in the frequency range from 90 to 100 GHz. In the volumetric model (Fig. 17), numbers 1 and 2 denote the corresponding microwave power input and output ports. The results of SWR and attenuation modelling showed that this waveguide transition in the frequency range from 90 to 100 GHz has an average SWR value not exceeding 1,2, an average attenuation of 0,5 dB, and is a reciprocal device, which determines its suitability for use in a flexible waveguide for MW communication with standard and oversized cross-sections.

The waveguide transition from DV to SSMW was included in the flexible waveguide model for MW communication with a standard cross-section



Fig. 16. Waveguide nodes of the LP: a – rectangular oversized metal waveguide; b – pyramidal waveguide transition
Рис. 16. Волноводные узлы ЛП: а – прямоугольные СРМВ; б – пирамидальный волноводный переход

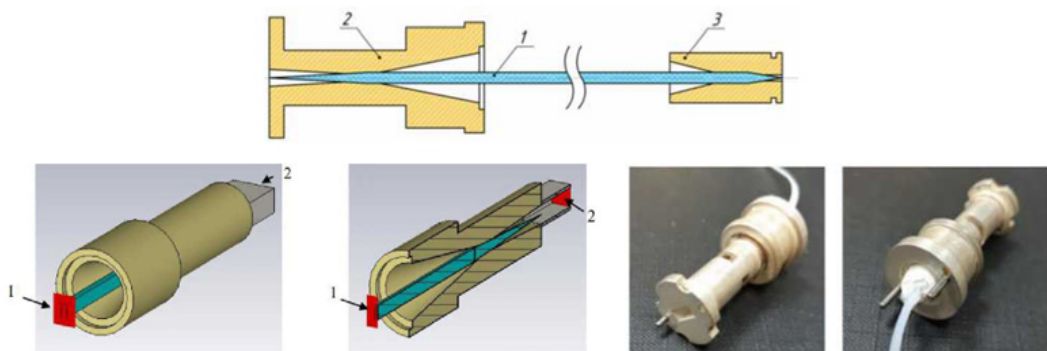


Fig. 17. Flexible waveguide device for communication of standard and oversized metallic waveguide sections, model of waveguide transition from dielectric waveguide to oversized metal waveguide in CST MWS and its experimental sample
Рис. 17. Устройство гибкого волновода для связи МВ стандартного и сверхразмерного сечений, модель волноводного перехода с ДВ на СРМВ в CST MWS и его экспериментальный образец

of $2,4 \times 1,2 \text{ mm}^2$ and an oversized cross-section of $7,2 \times 3,4 \text{ mm}^2$ with a fluoroplastic DV cross-section of $2,2 \times 1,0 \text{ mm}^2$. Experimental studies have shown that the total losses in a flexible waveguide with a waveguide length of 0,5 m do not exceed 1,1 dB, and in each of the waveguide transitions -0,3 dB.

Despite the possibility of bending, the weak point of such a waveguide (in terms of the impact of a direct shock wave) remains a rigid regular section containing a rectangular SSMW. However, when using flexible waveguides, it is possible to protect the SSMW from impact, thereby limiting the destroyed section to only part of the replaceable waveguide from the flexible waveguide assembly.

When transitioning to the sub-millimetre wavelength range, the task of minimising losses in the path

becomes even more acute. In the frequency range around 300 GHz, the loss tangent of F-4 fluoroplastic increases to $4 \cdot 10^{-4}$, and the attenuation coefficient per unit length of a waveguide with a cross-section of $0,9 \times 0,45 \text{ mm}^2$ is approximately 12 dB/m. Thus, with the required path length of at least 1,5 m, the use of a dielectric feeder line made of F-4 in the sub-mm range becomes impossible. The use of low-pressure polyethylene (HDPE) with $\text{tg}\delta \approx 2 \cdot 10^{-4}$ allows reducing line losses to 8 dB/m, which, however, is also insufficient for creating long lines. In this regard, the use of DV in the sub-mm range is limited to short sections as part of a combined feeder line, ensuring its flexibility and breakage when exposed to a shock wave.

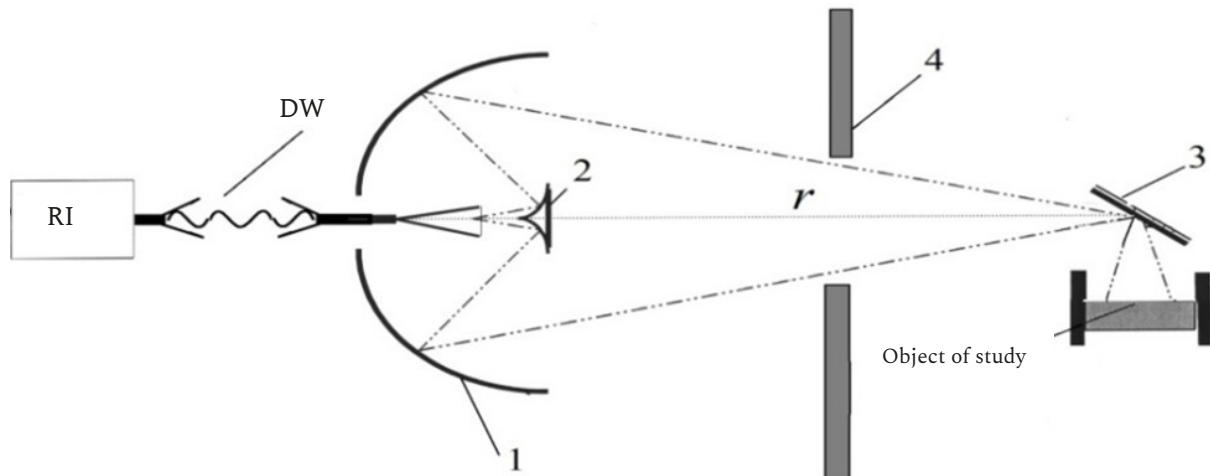


Fig. 18. Measurement scheme using quasi-optical antenna-feeder system
 Рис. 18. Схема измерений при использовании квазиоптической АФС

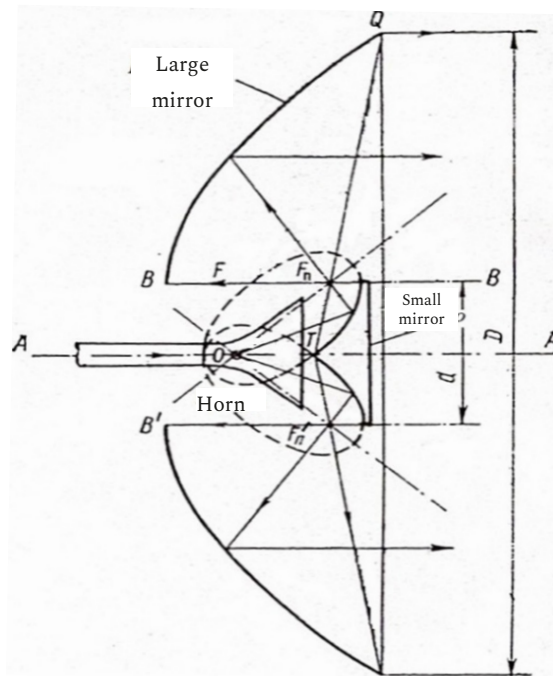


Fig. 19. Schematic diagram of a two-mirror antenna with split focus
 Рис. 19. Схема двухзеркальной антенны с расщепленным фокусом

In this case, only the SRM and waveguide are destroyed during the experiment, while the most complex components – horn transitions and waveguide flanges – remain suitable for further use.

A rectangular SSMW with a standard waveguide channel cross-section of $7,2 \times 3,4 \text{ mm}^2$ can be used on a long section ($\sim 1 \text{ m}$) of the combined feeder line. At $\lambda \approx 1 \text{ mm}$, the calculated losses in the SSMW are $0,8 \text{ dB/m}$ for the H_{10} mode and $0,5 \text{ dB/m}$ for the H_{01} mode. Based on this fact, it is advisable to select the H_{01} mode as the working mode of the waveguide.

The design of conical horn transitions intended for connecting the DV to the RI output waveguide with a cross-section of $0,9 \times 0,45 \text{ mm}^2$ and the SSMW is similar to that described above. Losses at each transition do not exceed 1 dB.

It is proposed to use the open end of the SSMW as the irradiator of the combined AFS, as it is the simplest to implement and has acceptable radiation characteristics. The results of numerical modelling showed that in the E-plane, the width of the irradiator's beam is $7,4^\circ$, and the beam width is minus

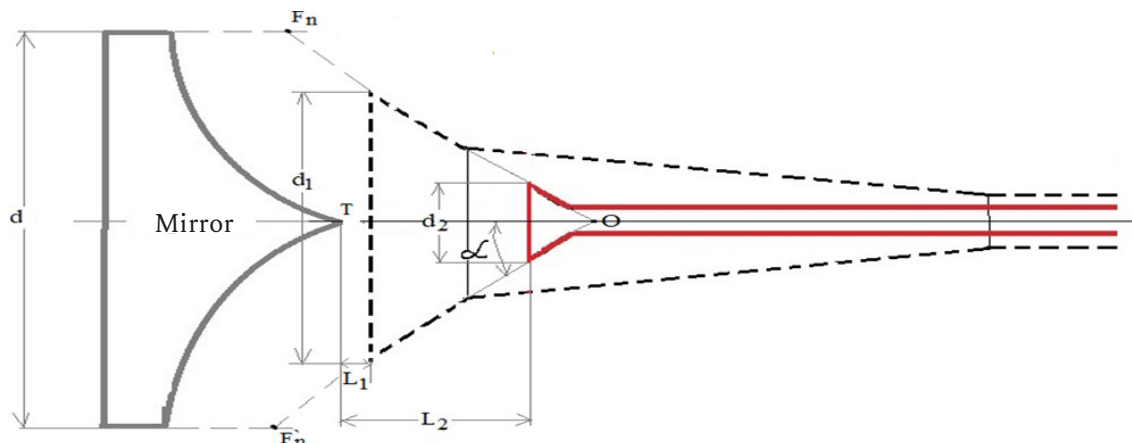


Fig. 20. Horn feed and its relative position relative to the small mirror: $\lambda_1 = 3.2$ mm (dashed line); $\lambda_2 = 1.06$ mm (solid line)
 Рис. 20. Рупорный облучатель и его взаимное расположение относительно малого зеркала: $\lambda_1 = 3,2$ мм (пунктирная линия); $\lambda_2 = 1,06$ мм (сплошная линия)

13,2 dB. In the H-plane, the beam width is $20,9^\circ$, and the beam width is minus 24,7 dB [25].

5. Quasi-optical AFS in the 3 mm and sub-millimetre ranges

Another variant of the AFS design is based on the formation of a wave beam in free space by an axisymmetric two-mirror long-focus antenna with an elliptical generatrix of a small mirror [26].

A specific feature of the use of AFS in RI is the need for the line of sight of the objects under study to coincide with their trajectory of movement. Therefore, to protect the mirror antenna from destruction during gas-dynamic experiments, a destructible flat mirror is introduced into the AFS, separating the optical axis of the antenna and the destruction vector, which coincides with the direction of movement of the object. The measurement diagram is shown in Fig. 18, where 1 is a large mirror, 2 is a small mirror, 3 is a flat mirror, 4 is the antenna explosion protection, and r is the distance from the aperture to the focus.

The antenna excites a quasi-optical waveguide system with a flat mirror, which allows, depending on the size and distance of the object under study, to redirect the incident beam and focus it on the object being diagnosed. A 40–60 mm long DV segment can be used as a damper for the RI connection to the antenna.

When analysing the operation of the antenna, a geometric-optical representation (ray interpretation of wave propagation) can be used, since the conditions of the near and intermediate zones are met: $r < 2D^2/\lambda$, where D is the antenna aperture. The width of the formed focal spot l at half the maximum radiation intensity is determined by Rayleigh's formula:

$l = 1,21\lambda r/D$, and the depth of field at 0,9 of the maximum corresponding to the focus for long-focus antennas is approximately equal to $(30-50)\lambda$. The focal length is equal to three aperture diameters D , and an aperture diameter of about 30 cm is sufficient for focusing at a distance of 1 m.

The essence of the quasi-optical antenna under consideration is well illustrated in Fig. 19, described in more detail in [27]. The minor focal axis B-B of the large mirror is made in the form of an axisymmetric cutout from an ellipsoid of revolution. The diameter of the small mirror d is determined by the condition of equality of the distance between the foci F_n and F_n' . The small mirror is made in the form of a cylinder, the end facing the illuminator of which is profiled as an axisymmetric cutout from an ellipsoid of revolution. One of its foci, O , lies on the optical axis of the antenna and must coincide with the phase centre of the horn radiator (RO).

The characteristics of the entire antenna are largely determined by the beam pattern of the primary source, the TR. In this case, the shape of the main

lobe in the sector of radiation of the small mirror, the steepness of the DN and SL outside the sector are crucial.

The following requirements are imposed on the PO to create an optimal field distribution at the antenna aperture:

- a clearly defined phase centre of the horn, which must coincide with the focus O of the small mirror along the antenna axis;
- axisymmetric main lobe in the E and H planes;
- the irradiation level of the outer edge of the small mirror should be no more than minus 13...15 dB from the maximum value of the main lobe of the directional pattern in order to avoid energy leakage

beyond the small mirror and to minimise diffraction effects at the edge.

These requirements are met by a phased conical horn with a break in the conical generatrix at an angle of 40–50° between the generatrix and the axis of symmetry. The phase centre of such horns lies at the mouth of the horn.

In a quasi-optical antenna designed for a specific frequency in the mm range, the mirror system can also be used at any other higher frequency. This is true provided that the horn radiator ensures the specified focus ratios F_n and O and meets the requirements for the radiator set out above.

Work [27] describes a quasi-optical antenna in the 3 mm band, previously developed at the RIMS, for radio interferometric diagnostics of gas-dynamic processes, which has a high spatial resolution of the order of the wavelength of the probing radiation. The diameters of its large D and small d mirrors are 320 mm and 20 mm, respectively. The antenna focuses radiation at a distance of 984 mm from the aperture with a resolution of 10,5 mm in the transverse coordinate and a depth of field (at the 0,9 level) of 100 mm.

Due to its broadband nature, the antenna mirror system can also operate in the submillimetre range, in particular at a wavelength of $\lambda = 1$ mm, but this requires the development of an appropriate RO equivalent to a 3 mm range irradiator in terms of electrical characteristics and design.

Using comparative numerical modelling of the RO in mm and sub-mm, the dimensions of the sub-mm range RO ($\lambda = 1,06$ mm) were evaluated. Fig. 20 shows the mm and sub-mm range irradiators and their relative positions with respect to the small mirror.

The RO contour for an operating frequency of 93,5 GHz ($\lambda_1 = 3,2$ mm) is shown (dotted line). The illuminator for an operating frequency of 282,3 GHz ($\lambda_2 = 1,06$ mm) is shown as a solid line.

The parameters of the 3 mm range are interrelated with the focal points of the large and small mirrors. The half-aperture angle α of the phased horn antenna is 45°. The diameter of the focal ring $F_n F'_n$ is equal to the diameter $d = 20$ mm of the small mirror. A horn with a near-symmetrical radiation pattern and an external edge of the small mirror with an irradiation level no more than minus 13 dB from the maximum radiation pattern is achieved with a horn aperture diameter d_1 equal to 13,5 mm.

For an RO operating at a wavelength $\lambda_2 = 1,06$ mm, in order to maintain the relationship between the geometric dimensions and the focal points of the mirrors, the angle α , the distance OT from the

phase centre O to the conical tip T of the small mirror, and the diameter d must be preserved. To achieve $\lambda_2 = 1,06$ mm, identical to the beam pattern of a 3 mm RO, the diameter of the horn aperture is selected to be $d_2 = 4,45$ mm. Accordingly, the distance L_2 from the horn aperture to the tip of the small mirror increases from 2,35 mm to 6,85 mm.

Numerical simulation of the radiation characteristics of both irradiators showed that at an operating frequency of 93,5 GHz, the original irradiator forms an almost symmetrical beam pattern. The beam width is -39° and 42,5° in the E and H planes, respectively. The irradiation level at the edge of the small mirror is no more than minus 20 dB (E-plane) and minus 13 dB (H-plane). The results of modelling the beam pattern of the RF for the submillimetre band AFS operating at a frequency of 282,3 GHz ($\lambda_2 = 1,06$ mm) show an almost complete coincidence of the beam patterns: the beam width of the developed RF was 37,3° and 44,4° in the E- and H-planes, respectively.

The irradiation level of the edge of the small mirror is no more than minus 25 dB and minus 13 dB in the corresponding planes [28]. The radiation characteristics of the two RO are identical, which will allow the proposed design to be used at a wavelength of $\lambda = 1,06$ mm for irradiating a three-millimetre two-mirror AFS system without recalculating the designs of elliptical surfaces.

Although quasi-optical AFS is technologically more complex, it allows for spatial resolution of the order of wavelength and minimises losses in the measuring path in both the mm and sub-mm wavelength ranges, which expands the diagnostic capabilities and increases the accuracy of measurements of gas-dynamic processes in the sub-mm wavelength range.

This version of the AFS requires complex adjustment and is only applicable if the antenna is protected from shock waves and shrapnel damage.

Conclusion

Currently, the radio interferometric diagnostic method is a unique non-contact method for diagnosing fast-moving processes, widely used to measure the motion parameters and electrophysical characteristics of substances. The article shows the advantages of the microwave method and considers a wide range of methods and schemes for constructing antenna-feeder systems for EHF radio interferometers, justifying the use of various types of AFS – dielectric, metallic, combined metal-dielectric, quasi-optical, depending on the task at hand and the operating frequency range.

References

1. A. L. Mikhailov, Ed. *Non-Disturbing Methods for Diagnostics of Fast-Flowing Processes*. Sarov: RFYaTs-VNIIEF, 2015. (In Russ.)
2. V. A. Kanakov et al., “The state and prospects of the development of microwave radio interferometry for diagnosis of gas dynamic processes,” *Antenny*, no. 1 (221), pp. 49–54, 2016, url: <https://elibrary.ru/item.asp?id=25680917>. (In Russ.)
3. A. L. Mikhaylov et al., “Some of the results of application in the IFV RFD-VNIIEF of radio interferometers of millimeter wavelengths for studying gas-dynamic processes,” *Ekstremal'nye sostoyaniya veshchestva. Detonatsiya. Udarnye volny*: tr. Mezhd. konf. VII Kharitonovskie tematicheskie nauchnye chteniya. Sarov, 14–18 March 2005. Sarov: RFYaTs-VNIIEF, pp. 649–654, 2005. (In Russ.)
4. V. M. Bel'skiy et al., “Microwave diagnosis of shock waves and detonation processes,” *Fizika gorenija i vzryva*, vol. 47, no. 6, pp. 29–41, 2011, url: https://sibran.ru/journals/issue.php?ID=120267&ARTICLE_ID=132478. (In Russ.)
5. V. F. Vzyatyshev, Yu. I. Orekhov, and A. G. Pankratov, “The wave water transition from the metal waveguide to the dielectric,” RU Patent 2557472, Jul. 20, 2015. (In Russ.)
6. E. Yu. Gaynulina and V. V. Shtykov, “Multi-moded mode of dielectric planar wave-water converters,” *Izvestiya vuzov. Fizika*, vol. 55, no. 8-3, pp. 5–10, 2012, url: <https://elibrary.ru/item.asp?id=18054069>. (In Russ.)
7. V. V. Shtykov et al., “Diffraction of sounding and information wave beams in the process of distribution and interaction,” *Extreme states of matter. Detonation. Shock waves*: tr. Int. conf. VIII Kharitonov Scientific Readings. Sarov, 14–18 March 2011. Sarov: RFYaTs-VNIIEF, pp. 694–698, 2011. (In Russ.)
8. A. G. Pankratov, A. V. Rodionov, E. Yu. Gaynulina, V. N. Khvorostin, and V. F. Vzyatyshev, “Dielectric conical emitter,” RU Patent 2485644, 20 June 2013. (In Russ.)
9. V. F. Vzyatyshev, E. Yu. Gaynulina, N. A. Makarychev, and Yu. I. Orekhov, “Planning emitter,” RU Patent 2447552, 10 April 2012. (In Russ.)
10. V. F. Vzyatyshev, E. Yu. Gaynulina, Yu. I. Orekhov, and A. V. Rodionov, “Dielectric planar emitter,” RU Patent 2515700, 20 May 2014. (In Russ.)
11. V. F. Vzyatyshev, S. A. Klyachin, and E. Yu. Gaynulina, “Diphysational KVH wave-water converters on open multi-muddy dielectric wavelengths: phenomena physics in the near zone and relevant applications,” *Radiolokatsiya i radiosvyaz'*: tr. III Vserossiyskoy nauch.-tekhn. konf. Moscow, 26–30 October 2009. Moscow: IRE RAN RF, pp. 186–187, 2009, url: <http://jre.cplire.ru/jre/library/3conference/pdfes/t009.pdf>. (In Russ.)
12. E. Yu. Gaynulina, “Amplitude-phase distribution of fields on a multi-moded dielectric waveguide for radio interferometric diagnostics of objects,” cand. tech. sciences. dissertation, Moscow, 2014. (In Russ.)
13. V. V. Shtykov, E. Yu. Gaynulina, and A. V. Nazarov, “Implementation of the multi-moded wave regime for the synthesis of AFR dielectric planar irradiators,” *SVCh-tehnika i telekommunikatsionnye tekhnologii*: tr. 24th International Conference “KryMiKo 2014”. Sevastopol, 7–13 September 2014. Sevastopol: Veber, pp. 623–624, 2014. (In Russ.)
14. V. V. Shtykov, E. Yu. Gaynulina, A. V. Nazarov, A. A. Sedov, and V. N. Khvorostin, “Planning dielectric emitter,” RU Patent 2578660 C1, 27 March 2016. (In Russ.)
15. E. Yu. Gaynulina, N. S. Kornev, and A. V. Nazarov, “Study of the possibility of creating a small-sized antenno-phased radio interferometer,” *Information Systems and Technologies: Proceedings of the XXIII International Scientific and Technical Conference dedicated to the 100th anniversary of NGTU IST-2017*. Nizhniy Novgorod, 21 April 2017. Nizhniy Novgorod: NGTU im. R.E. Alekseeva, pp. 1062–1067, 2017, url: <https://www.elibrary.ru/item.asp?id=41200731>. (In Russ.)
16. V. F. Vzyatyshev et al., “Diagnosis of gas-dynamic processes with microwave interferometers with sounding of objects with gowsk wave beams,” *Extreme states of matter. Detonation. Shock waves*: tr. Int. conf. XVII Kharitonov thematic scientific readings. Sarov, 23–27 March 2015. Sarov: RFYaTs-VNIIEF, pp. 810–814, 2015. (In Russ.)
17. K. V. Mineev et al., “The exciting systems of the AFC band with small losses for use in diagnostic devices of rapidly flowing gas-dynamic processes,” *Budushchee tekhnicheskoy nauki*: sb. mat. XV Mezhd. molod. nauch.-tekhn. konf. Nizhniy Novgorod, 27 May 2016. Nizhniy Novgorod: NGTU im. R.E. Alekseeva, pp. 404–405, 2016. (In Russ.)
18. C. Yeh and F. I. Shimabukuro, *The Essence of Dielectric Waveguides*. New York: Springer, 2008.
19. A. A. Kostenko, “Quasioptics: Historical prerequisites and modern development trends,” *Radiofizika i radioastronomia*, no. 3, pp. 221–246, 2000. (In Russ.)
20. L. B. Knyaz'kov and N. V. Ruzhentsev, “The fenodielectric lenses of gearboxes of the millimetre and submillimetre range of wavelengths,” *Pis'ma v zhurnal tekhnicheskoy fiziki*, no. 20, pp. 59–64, 2008, url: <https://journals.iofe.ru/articles/13844>. (In Russ.)
21. V. B. Steinshleiger, Ed. *Low-Loss Waveguide Transmission Lines*. Moscow: Izdatel'stvo inostrannoy literature, 1960. (In Russ.)
22. Yu. N. Kazantsev and O. A. Kharlashkin, “Round waves of the class ‘Having hollow dielectric canal’,” *Radiotekhnika i elektronika*, no. 8, pp. 1441–1450, 1984. (In Russ.)
23. V. V. Biryukov, K. V. Mineev, and A. V. Nazarov, “Accounting for roughnesses of shielding surfaces of the waves,” *Physics and technical applications of wave processes: proceedings of the XIV International scientific and technical conference*. Samara, 22–24 November 2016. Kazan: OOO “16Print”, pp. 143, 2016. (In Russ.)

24. E. Yu. Gaynulina, N. S. Kornev, K. V. Mineev, A. V. Nazarov, Yu. I. Orekhov, and Yu. A. Svetlakov, "A flexible waveguide for the connection of metal waves of standard and superior sections," RU Patent 2657318, 13 June 2018. (In Russ.)
25. E. Yu. Gaynulina et al., "Antenna-phased system of the radio interferometer of the submillimetre range," *Mathematical Methods in Technology and Engineering*, no. 5, pp. 66-72, 2023, url: <https://elibrary.ru/item.asp?id=54118756>. (In Russ.)
26. G. Z. Ayzenberg, V. G. Yampol'skiy, and O. N. Tereshin, *Antennas VHF. Part 2. Moscow: Svyaz'*, 1977. (In Russ.)
27. V. A. Kanakov et al., "UHF antennas for radio vision systems," *Antenny*, no. 5 (108), pp. 13-16, 2006, url: <https://elibrary.ru/item.asp?id=9200087>. (In Russ.)
28. E. Yu. Gaynulina et al., "Options for constructing an antenno-feeding system for the tasks of radio interferometric measurements in the submillimetre range," *Vestnik MGTU im. N.E. Baumana. Ser. Instrument Engineering*, no. 2 (147), pp. 37-54, 2024, url: <https://elibrary.ru/item.asp?id=67964696>. (In Russ.)

Information about the Authors

Ekaterina Yu. Gaynulina, Candidate of Technical Sciences, senior researcher of the Department of Measuring Systems Development, Russian Federal Nuclear Centre – All-Russian Research Institute of Experimental Physics, Sarov, Nizhny Novgorod Region, Russia. Research interests: theory of wave processes, microwave and antenna technology.

E-mail: okatrin@list.ru

ORCID: <https://orcid.org/0000-0002-8554-4116>

SPIN code (eLibrary): 1154-1346

AuthorID (eLibrary): 889563

ResearcherID (WoS): O-8311-2016

Vladimir N. Ikonnikov, Candidate of Physical and Mathematical Sciences, senior researcher at the Department of Measuring Systems Development, Russian Federal Nuclear Centre – All-Russian Research Institute of Experimental Physics, Sarov, Nizhny Novgorod Region, Russia.

Research interests: microwave probing, EHF technology, antenna-feeder systems, radio photonics.

Email: ikonnikov-vn@yandex.ru

ORCID: <https://orcid.org/0000-0001-9455-4001>

SPIN code (eLibrary): 5415-6868

AuthorID (eLibrary): 923042

ResearcherID (WoS): IST-7258-2023

Nikolay S. Kornev, head of the Department of Measuring Systems Development, Russian Federal Nuclear Centre – All-Russian Research Institute of Experimental Physics, Sarov, Nizhny Novgorod Region, Russia. *Research interests:* radiophysics, microwave and antenna technology.

E-mail: kornev15@rambler.ru

ORCID: <https://orcid.org/0000-0002-7848-3917>

SPIN code (eLibrary): 9853-6653

AuthorID (eLibrary): 998470

Andrey V. Nazarov, Candidate of Technical Sciences, deputy chief designer – head of the Department of Radioelectronic Systems Development, Russian Federal Nuclear Centre – All-Russian Research Institute of Experimental Physics, Sarov, Nizhny Novgorod Region, Russia.

Research interests: electrodynamics, radar, antennas, techniques of microwave and optical ranges.

Email: nazarov52@mail.ru

ORCID: <https://orcid.org/0000-0002-0261-1724>

SPIN code (eLibrary): 6516-0650

AuthorID (eLibrary): 615493

ResearcherID (WoS): R-9919-2016

Yuriy I. Orekhov, Doctor of Technical Sciences, chief researcher of the Department of Advanced Research and Development, Russian Federal Nuclear Centre – All-Russian Research Institute of Experimental Physics, Sarov, Nizhny Novgorod Region, Russia.

Research interests: radiophysics, microwave and antenna technology.

SPIN code (eLibrary): 5355-0380

AuthorID (eLibrary): 553962

Физика волновых процессов и радиотехнические системы 2025. Т. 28, № 1. С. 56-75

DOI [10.18469/1810-3189.2025.28.1.56-75](https://doi.org/10.18469/1810-3189.2025.28.1.56-75)

УДК 537.87

Оригинальное исследование

Дата поступления 28 ноября 2024

Дата принятия 28 декабря 2024

Дата публикации 31 марта 2025

Антенно-фидерные системы КВЧ-радиоинтерферометров

E.Yu. Гайнулина , B.N. Иконников ,
H.S. Корнев , A.B. Назаров , Ю.И. Орехов

Российский федеральный ядерный центр –
Всероссийский научно-исследовательский институт экспериментальной физики
607188, Россия, Нижегородская обл., г. Саров,
пр. Мира, 37

Аннотация – Обоснование. Развитие микроволнового метода исследования ударно-волновых и детонационных процессов с применением радиоинтерферометров требует разработки антенно-фидерных систем с учетом специфики газодинамических экспериментов. Цель. Проектирование антенно-фидерных систем радиоинтерферометров миллиметрового и субмиллиметрового диапазонов длин волн, разработка вариантов построения фидерных линий и зондирующих устройств. Методы. Приводятся результаты численного моделирования в CST MWS, теоретических расчетов и экспериментальных исследований антенно-фидерных систем радиоинтерферометров, подтверждающие эффективность предложенных технических решений. Результаты. Приведены требования к антенно-фидерной системе как составной части радиоинтерферометра. Обоснованы преимущества диэлектрических излучателей, предложены диэлектрические излучатели планарного типа. Показаны малогабаритные антенно-фидерные системы с диэлектрическими вставками, нашедшие свое применение в задачах зондирования в замкнутых объемах. С целью снижения потерь в фидерной линии и построения линий длиной до нескольких метров исследованы антенно-фидерные системы на прямоугольных сверхразмерных металлических волноводах, в том числе предложены пирамидальные рупорные переходы со стандартного сечения волновода на сверхразмерное сечение, комбинированная фидерная линия с использованием гибкого диэлектрического волновода для связи волновода стандартного и сверхразмерного сечения. Рассмотрена квазиоптическая двухзеркальная антенна, обладающая высоким пространственным разрешением и минимальными потерями. Заключение. В статье показаны преимущества микроволнового метода диагностики, представлены различные способы и схемы построения фидерных линий и обосновано применение типов зондирующих устройств (излучателей) в зависимости от решаемой задачи и диапазона рабочих частот.

Ключевые слова – радиоинтерферометр; антенно-фидерная система; зондирующее устройство; диэлектрический волновод; сверхразмерный волновод; квазиоптическая антенна.

✉ okatrin@list.ru (Гайнулина Екатерина Юрьевна)



©Гайнулина Е.Ю. и др., 2025

Список литературы

1. Невозмущающие методы диагностики быстропротекающих процессов / под. ред. д.т.н. А.Л. Михайлова. Саров: РФЯЦ-ВНИИЭФ, 2015. 322 с.
2. Состояние и перспективы развития микроволновой радиоинтерферометрии для диагностики газодинамических процессов / В.А. Канаков [и др.] // Антенны. 2016. № 1 (221). С. 49–54. URL: <https://elibrary.ru/item.asp?id=25680917>
3. Некоторые результаты применения в ИФВ РФЯЦ-ВНИИЭФ радиоинтерферометров миллиметрового диапазона длин волн для изучения газодинамических процессов / А.Л. Михайлов [и др.] // Экстремальные состояния вещества. Детонация. Ударные волны: тр. Межд. конф. VII Харитоновские тематические научные чтения. Саров, 14–18 марта 2005 г. Саров: РФЯЦ-ВНИИЭФ, 2005. С. 649–654.
4. Микроволновая диагностика ударно-волновых и детонационных процессов / В.М. Бельский [и др.] // Физика горения и взрыва. 2011. Т. 47, № 6. С. 29–41. URL: https://sibran.ru/journals/issue.php?ID=120267&ARTICLE_ID=132478
5. Патент RU 2557472. Волноводный переход от металлического волновода к диэлектрическому / В.Ф. Взятышев, Ю.И. Орехов, А.Г. Панкратов и др.; 20.07.2015.
6. Гайнулина Е.Ю., Штыков В.В. Многомодовый режим диэлектрических планарных волноводно-пучковых преобразователей // Известия вузов. Физика. 2012. Т. 55, № 8-3. С. 5–10. URL: <https://elibrary.ru/item.asp?id=18054069>
7. Дифракция зондирующих и информационных волновых пучков в процессе распространения и взаимодействия / В.В. Штыков [и др.] // Экстремальные состояния вещества. Детонация. Ударные волны: тр. Межд. конф. VIII Харитоновские научные чтения. Саров, 14–18 марта 2011 г. Саров: РФЯЦ-ВНИИЭФ, 2011. С. 694–698.
8. Патент RU 2485644. Диэлектрический конический излучатель / А.Г. Панкратов, А.В. Родионов, Е.Ю. Гайнулина, В.Н. Хворостин, В.Ф. Взятышев; 20.06.2013.
9. Патент RU 2447552. Планарный излучатель / В.Ф. Взятышев, Е.Ю. Гайнулина, Н.А. Макарычев, Ю.И. Орехов; 10.04.2012.
10. Патент RU 2515700. Диэлектрический планарный излучатель / В.Ф. Взятышев, Е.Ю. Гайнулина, Ю.И. Орехов, А.В. Родионов; 20.05.2014.
11. Взятышев В.Ф., Клячин С.А., Гайнулина Е.Ю. Дифракционные КВЧ волноводно-пучковые преобразователи на открытых многомодовых диэлектрических волноводах: физика явлений в ближней зоне и актуальные применения // Радиолокация и радиосвязь: тр. III Всероссийской науч.-техн. конф. Москва, 26–30 октября 2009 г. М.: ИРЭ РАН РФ, 2009. С. 186–187. URL: <http://jre.cplire.ru/jre/library/3conference/pdffiles/t009.pdf>
12. Гайнулина Е.Ю. Преобразователи амплитудно-фазового распределения полей на многомодовом диэлектрическом волноводе для радиоинтерферометрической диагностики объектов: дис. ... канд. техн. наук. Москва, 2014. 164 с.
13. Штыков В.В., Гайнулина Е.Ю., Назаров А.В. Реализация многомодового режима волн для синтеза АФР диэлектрических планарных облучателей // СВЧ-техника и телекоммуникационные технологии: тр. 24-й Межд. конф. «КрыМиКо 2014». Севастополь, 7–13 сентября 2014 г. Севастополь: Вебер, 2014. С. 623–624.

14. Патент RU 2578660 С1. Планарный диэлектрический излучатель / В.В. Штыков, Е.Ю. Гайнулина, А.В. Назаров, А.А. Седов, В.Н. Хворостин; 27.03.2016.
15. Гайнулина Е.Ю., Корнев Н.С., Назаров А.В. Исследование возможности создания малогабаритной антенно-фидерной системы КВЧ радиоинтерферометра // Информационные системы и технологии: сб. мат. докл. XXIII Межд. науч.-техн. конф. к 100-летию НГТУ ИСТ-2017. Нижний Новгород, 21 апреля 2017 г. Н. Новгород: НГТУ им. Р.Е. Алексеева, 2017. С. 1062–1067. URL: <https://www.elibrary.ru/item.asp?id=41200731>
16. Диагностика газодинамических процессов микроволновыми интерферометрами с зондированием объектов гауссовыми волновыми пучками / В.Ф. Взятышев [и др.] // Экстремальные состояния вещества. Детонация. Ударные волны: тр. Межд. конф. XVII Харитоновские тематические научные чтения. Саров, 23–27 марта 2015 г. Саров: РФЯЦ-ВНИИЭФ, 2015. С. 810–814.
17. Волноведущие системы КВЧ-диапазона с малыми потерями для применения в устройствах диагностики быстропротекающих газодинамических процессов / К.В. Минеев [и др.] // Будущее технической науки: сб. мат. XV Межд. молод. науч.-техн. конф. Нижний Новгород, 27 мая 2016 г. Н. Новгород: НГТУ им. Р.Е. Алексеева, 2016. С. 404–405.
18. Yeh C., Shimabukuro F.I. The Essence of Dielectric Waveguides. New York: Springer, 2008. 528 р.
19. Костенко А.А. Квазиоптика: исторические предпосылки и современные тенденции развития // Радиофизика и радиоастрономия. 2000. № 3. С. 221–246.
20. Князьков Л.Б., Руженцев Н.В. Пенодиэлектрическая линзовая линия передач миллиметрового и субмиллиметрового диапазона длин волн // Письма в журнал технической физики. 2008. № 20. С. 59–64. URL: <https://journals.ioffe.ru/articles/13844>
21. Волноводные линии передачи с малыми потерями / под. ред. В.Б. Штейншлейгера. М.: Издательство иностранной литературы, 1960. 480 с.
22. Казанцев Ю.Н., Харлашкин О.А. Круглые волноводы класса «полый диэлектрический канал» // Радиотехника и электроника. 1984. № 8. С. 1441–1450.
23. Бирюков В.В., Минеев К.В., Назаров А.В. Учет шероховатостей экранирующих поверхностей волноводов // Физика и технические приложения волновых процессов: мат. XIV Межд. науч.-техн. конф. Самара, 22–24 ноября 2016 г. Казань: ООО «16Принт», 2016. С. 143.
24. Патент RU 2657318. Гибкий волновод для связи металлических волноводов стандартного и сверхразмерного сечений / Е.Ю. Гайнулина, Н.С. Корнев, К.В. Минеев, А.В. Назаров, Ю.И. Орехов, Ю.А. Светлаков; 13.06.2018.
25. Антенно-фидерная система радиоинтерферометра субмиллиметрового диапазона / Е.Ю. Гайнулина [и др.] // Математические методы в технологиях и технике. 2023. № 5. С. 66–72. URL: <https://elibrary.ru/item.asp?id=54118756>
26. Айзенберг Г.З., Ямпольский В.Г., Терешин О.Н. Антенны УКВ. Ч. 2. М.: Связь, 1977. 288 с.
27. Антенны КВЧ-диапазона для систем радиовидения / В.А. Канаков [и др.] // Антенны. 2006. № 5 (108). С. 13–16. URL: <https://elibrary.ru/item.asp?id=9200087>
28. Варианты построения антенно-фидерной системы для задач радиоинтерферометрических измерений в субмиллиметровом диапазоне / Е.Ю. Гайнулина [и др.] // Вестник МГТУ им. Н.Э. Баумана. Сер. Приборостроение. 2024. № 2 (147). С. 37–54. URL: <https://elibrary.ru/item.asp?id=67964696>

Информация об авторах

Гайнулина Екатерина Юрьевна, кандидат технических наук, старший научный сотрудник НИО разработки измерительных систем Российского федерального ядерного центра – Всероссийский научно-исследовательский институт экспериментальной физики, г. Саров, Нижегородская область, Россия.

Область научных интересов: теория волновых процессов, СВЧ-техника, антенная техника.

E-mail: okatrin@list.ru

ORCID: <https://orcid.org/0000-0002-8554-4116>

SPIN-код (eLibrary): 1154-1346

AuthorID (eLibrary): 889563

ResearcherID (WoS): O-8311-2016

Иконников Владимир Николаевич, кандидат физико-математических наук, старший научный сотрудник НИО разработки измерительных систем Российского федерального ядерного центра – Всероссийский научно-исследовательский институт экспериментальной физики, г. Саров, Нижегородская область, Россия.

Область научных интересов: микроволновое зондирование, КВЧ-техника, антенно-фидерные системы, радиофотоника.

E-mail: ikonnikov-vn@yandex.ru

ORCID: <https://orcid.org/0000-0001-9455-4001>

SPIN-код (eLibrary): 5415-6868

AuthorID (eLibrary): 923042

ResearcherID (WoS): IST-7258-2023

Корнев Николай Сергеевич, начальник НИО разработки измерительных систем Российского федерального ядерного центра – Всероссийский научно-исследовательский институт экспериментальной физики, г. Саров, Нижегородская область, Россия.

Область научных интересов: радиофизика, СВЧ-техника, антенная техника.

E-mail: korneff15@rambler.ru

ORCID: <https://orcid.org/0000-0002-7848-3917>

SPIN-код (eLibrary): 9853-6653
AuthorID (eLibrary): 998470

Назаров Андрей Викторович, кандидат технических наук, заместитель главного конструктора – начальник НИО разработки радиоэлектронных систем Российского федерального ядерного центра – Всероссийский научно-исследовательский институт экспериментальной физики, г. Саров, Нижегородская область, Россия.

Область научных интересов: электродинамика, радиолокация, антенны, техника СВЧ-, КВЧ- и оптического диапазонов.
E-mail: nazarov52@mail.ru
ORCID: <https://orcid.org/0000-0002-0261-1724>
SPIN-код (eLibrary): 6516-0650
AuthorID (eLibrary): 615493
ResearcherID (WoS): R-9919-2016

Орехов Юрий Иванович, доктор технических наук, главный научный сотрудник отдела перспективных научных исследований и разработок Российского федерального ядерного центра – Всероссийский научно-исследовательский институт экспериментальной физики, г. Саров, Нижегородская область, Россия.

Область научных интересов: радиофизика, СВЧ-техника, антенная техника.
SPIN-код (eLibrary): 5355-0380
AuthorID (eLibrary): 553962